

Frequency-dependent specific heat in quantum supercooled liquids: A mode-coupling study

Ankita Das*, Eran Rabani†, Kunimasa Miyazaki‡, and Upendra Harbola*

**Inorganic and Physical Chemistry,*

Indian Institute of Science, Bangalore 560012, India.

† Department of Chemistry, University of California,

and Materials Sciences Division, Lawrence Berkeley National Laboratory,

Berkeley, California 94720, United States;

The Sackler Center for Computational Molecular and Materials Science,

Tel Aviv University, Tel Aviv 69978, Israel.

‡Department of Physics, Nagoya University, Nagoya 464-8602, Japan and

a) Author to whom correspondence should be addressed: ankitadas@iisc.ac.in

Abstract

Frequency-dependence of specific heat in supercooled hard sphere liquid is computed using quantum mode-coupling theory (QMCT). Mode-coupling equations are solved using recently proposed perturbative method that allows to study relaxation in the moderate quantum regime where quantum effects assist liquid to glass transition. Zwanzig's formulation is used to compute the frequency-dependent specific heat in supercooled state using dynamical information from QMCT. Specific heat shows strong variation as the quantumness of the liquid is changed, which becomes more significant as density is increased. It is found that, near the transition point, different dynamical modes contribute to the specific heat in the classical and the quantum liquids.

I. INTRODUCTION

The glass transition has historically been viewed as a second-order phase transition [1, 2] involving a change in the specific heat of supercooled liquids, while the volume and entropy do not show any marked difference during the transition. Liquid-like modes that contribute to the measured thermodynamic quantities [3] (such as specific heat, thermal expansion coefficient, compressibility etc.) near the glass transition are no longer able to equilibrate on the experimental time scales. In order to understand the complex relaxation behavior in supercooled liquids, several studies have investigated the response of a supercooled system to energy fluctuation, known as frequency dependence of specific heat in supercooled liquids [4-6].

The study of specific heat $C(T)$ in supercooled liquids is interesting as it is directly related to Kauzmann paradox [7]. Entropy of the liquid, defined thermodynamically as the integral $\int dTC(T)/T$, is greater than the crystal entropy at the melting point. As Kauzmann experimentally noted [7], configurational entropy in supercooled liquids falls rapidly as temperature is decreased and, if continued, it will become less than that of the crystal entropy at finite temperature (so called Kauzmann temperature, T_K) which is unphysical. One resolution of the Kauzmann paradox is to say that there must be a phase transition before the configurational entropy of the supercooled liquid becomes lesser than that of crystal. This implies that at a temperature $T(> T_K)$, the dynamics must get arrested, defined as the glass transition temperature (T_G). Recent simulation study [8] has been able to achieve deeply supercooled states, even lower than what has been realized in experiments, and successfully confirming the step decrease in entropy near the glass transition.

In 1985 Birge and Nagel [9] developed an experimental technique to study the dynamic response in supercooled liquids (propylene and glycerol) and obtained specific heat as function of frequency, famously known as “spectroscopy of specific heat”. In order to understand the origin of the frequency dependence of the specific heat, Oxtoby [10] analyzed the Birge and Nagel experiment based on generalized hydrodynamic theory by including a new internal mode relaxing on a time scale of hydrodynamic modes. Later, Zwanzig [11] argued that even without introducing any internal mode the experimental observation of Birge and Nagel could be well explained with generalized hydrodynamics. Zwanzig showed that experimentally what is measured as the frequency-dependent specific heat is related to

frequency-dependent longitudinal viscosity. Thus diverging viscosity in supercooled state is related to the frequency-dependent specific heat.

Mode-coupling theory (MCT) is based on generalized hydrodynamic approach which has been used successfully to study relaxation dynamics of glass forming materials using only static property such as temperature, density, and microscopic structure as input [12–15]. MCT has been applied to study the relation between dynamics of density fluctuation and frequency-dependent specific heat in classical supercooled liquids [16]. Although, most of MCT applications have been in the classical regime, there are interesting examples, where clear deviations from classical predictions have been attributed to quantum tunneling [17–19]. To understand the role of quantum effects on the dynamics of supercooled liquids, quantum mode-coupling theory (QMCT) has been formulated [20, 21]. In a recent simulation study [22] on vitrification of supercooled water, it has been shown that quantum effects play an important role in determining the frequency-dependent specific heat of water as well as ice.

In the present work we focus to study how the quantum fluctuations affect the frequency-dependent specific heat in supercooled liquids. We apply QMCT to compute structural relaxation in the moderate quantum regime. Zwanzig’s approach is used to compute the frequency-dependent specific heat using QMCT results for dynamics as inputs. In order to solve the dynamical QMCT equations we use a recently proposed [23] perturbation method which allows us to study the dynamics in the supercooled quantum liquids. The quantum effects are found to become increasingly important as the density is increased. At fixed density, slower modes start to contribute more to the specific heat as the quantumness increases.

In the next section we define frequency-dependent specific heat and present some essentials of QMCT which will be used in computing the frequency-dependent specific heat. In Sec. III we discuss our results. We conclude in Sec. IV.

II. SPECIFIC HEAT AND QMCT

In order to define specific heat, we use standard hydrodynamic equations [24] where mass density, momentum density and energy density are the dynamic variables of interest. As shown by Zwanzig [11], using generalized hydrodynamic equations for these variables, the

following generalized Fourier heat equation can be obtained [16],

$$i\omega\delta T(q, \omega) = -q^2\chi(q, \omega)\delta T(q, \omega), \quad (1)$$

where $\delta T(q, \omega)$ is the temperature fluctuation at wavelength q with frequency ω , $\chi(q, \omega) = \frac{\kappa}{[\rho_0 c_p(q, \omega)]}$ is thermal diffusivity, κ is thermal conductivity, ρ_0 is average mass density of the system. $c_p(q, \omega)$ is the frequency (ω) and wave-vector (q) dependent specific heat, defined as :

$$c_p(q, \omega) = c_v \left[1 + (\gamma_q - 1) \frac{1}{1 + i\omega\Gamma(q, \omega)} \right], \quad (2)$$

where $\gamma_q = \frac{c_p(q)}{c_v}$, c_v is specific heat at constant volume and $\Gamma(q, \omega)$ is normalized longitudinal viscosity. It is to be emphasized that the form of the hydrodynamic Eqs. (1) and (2) remain same for classical and quantum systems [25], the quantum signatures are included through the transport coefficients. Equation (2) can be rearranged to define normalized frequency-dependent specific heat $C_p(q, \omega) = \frac{c_p(q, \omega) - c_v}{c_p(q) - c_v} = \frac{1}{1 + i\omega\Gamma(q, \omega)}$, so that $C_p(q, 0) = 1$ for all q . For realistic systems such as liquid polyvalent metals like Ga, Cd, Zn, which can be approximated as hard-sphere (HS) system, c_v lies close to $3NK_B$, with the ratio c_p/c_v in the range (1.08 – 1.25) [26, 27]. Clearly, Eq. (2) suggests that $C_p(q, \omega)$ is complex in nature, where the real part corresponds to the propagation of heat fluctuations through the system and the imaginary part contains information of the important modes that contribute to heat absorption. In order to compute the $C_p(q, \omega)$ we need to evaluate $\Gamma(q, \omega)$ for the quantum system. Viscosity gives a direct measure of the system's resistance to flow when shear stress is applied. Viscosity is intimately related to the relaxation time of density correlation. Slower relaxation of the density correlation is reflected through higher viscosity in the system. The $\Gamma(q, \omega)$ is related to the memory kernel, $M(q, t)$, and the characteristic frequency of the system, Ω_q (to be discussed later) as [16]

$$\Gamma(q, \omega) = \frac{1}{\Omega_q^2} \int_0^\infty dt e^{i\omega t} M(q, t). \quad (3)$$

The real part of $\Gamma(q, \omega)$ provides information of the liquid-like viscous behavior in the system and the imaginary part corresponds to the solid-like elastic property of the system [24]. The memory kernel, $M(q, t)$ [23, 28] is evaluated using QMCT as described below.

QMCT is used to study the relaxation dynamics in simple liquids characterized in terms

of the relaxation of density correlation function [21, 28]

$$C_{\rho\rho}(q, t) = \frac{1}{N} \langle \hat{\rho}(-q, 0) \hat{\rho}(q, t) \rangle \quad (4)$$

where density operator is $\hat{\rho}(q) = \sum_{i=1}^N e^{iq \cdot \hat{r}_i}$, N is the total number of particles, \hat{r}_i is position vector of the i^{th} particle and $\langle \dots \rangle$ denotes quantum mechanical ensemble average. Due to difficulty in computing directly the full quantum mechanical correlation, ring polymer approach [29] is used to calculate Kubo-transformed correlation function,

$$\tilde{C}_{\rho\rho}(q, t) = \frac{1}{N\beta\hbar} \int_0^{\beta\hbar} d\lambda \langle C_{\rho\rho}(q, t + i\lambda) \rangle, \quad (5)$$

where $\beta = \frac{1}{k_B T}$, k_B is Boltzmann constant and \hbar is the Planck's constant. The Kubo-transformed correlation is related to the quantum correlation via the well known relation [30].

Time evolution of $\tilde{C}_{\rho\rho}$ is given in terms of nonlinear integro-differential equation given in Refs. [21, 28],

$$\frac{d^2 \tilde{C}_{\rho\rho}(q, t)}{dt^2} + \Omega_q^2 \tilde{C}_{\rho\rho}(q, t) + \int_0^t dt' M(q, t - t') \frac{d\tilde{C}_{\rho\rho}(q, t')}{dt'} = 0, \quad (6)$$

where $\Omega_q^2 = \frac{q^2}{m\beta\tilde{S}(q)}$, m denotes the particle mass and $\tilde{S}(q)$ is the zero-time Kubo-transformed density correlation.

In order to quantify quantumness in the system, we use parameter $\Lambda^* = \frac{\hbar}{\sqrt{m\sigma^2 K_B T}}$ which is the ratio of particle thermal wavelength and its size σ . The quantum fluctuations become important with gradual increase in Λ^* . At $\Lambda^* \rightarrow 0$ limit the QMCT reduces to the classical one [31]. For short times, dynamics of $\tilde{C}_{\rho\rho}(q, t)$ is mainly governed by the characteristic frequency Ω_q of the system. However, as time increases the memory term contributes through renormalizing the viscosity of the system in a non-linear manner; consequently, the dynamics of $\tilde{C}_{\rho\rho}(q, t)$ slows down.

To calculate $\Gamma(q, \omega)$ using Eq. (3), we require to solve Eq. (6) self-consistently along with the memory function. The memory function has been derived in Ref. [28] in the frequency domain. However, a direct implementation of the full memory function in computing the supercooled dynamics using self-consistent method becomes numerically very challenging.

To overcome this difficulty, we have recently proposed a perturbative approach [23] which expresses the memory function perturbatively in Λ^* (Eq. (11) in ref. [23]) directly in the time-domain which has been much easier to use in numerical calculations for moderate quantum regime ($\Lambda^* < 0.1$).

III. RESULTS

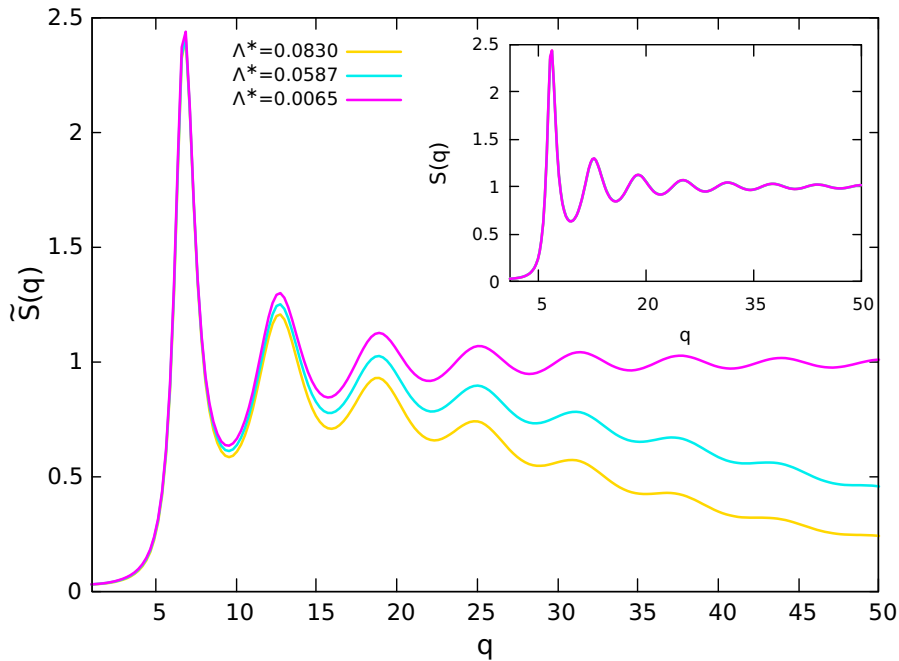


Figure 1: $\tilde{S}(q)$ for $\eta = 0.445$ for $\Lambda^* = 0.0065, 0.0587$ and 0.0830 . Inset: $S(q)$ for the same Λ^* values with no significant differences. q is given in the units of σ^{-1} .

The QMCT equations are solved self-consistently for a one-component HS system. The static structure factor $S(q)$ for HS supercooled liquid are generated by solving RISM [24] equations with PY [32] closure. $\tilde{S}(q)$, which is needed to solve Eq. (6), is generated using the approximation [28], $\tilde{S}(q) \approx \frac{2S(q)}{\beta\hbar\Omega_q\Delta n(\Omega_q)}$, where $\Delta n(\Omega_q) = n(\Omega_q) - n(-\Omega_q)$ and the Bose distribution function $n(\Omega_q) = \frac{1}{e^{\beta\hbar\Omega_q} - 1}$, shown in Fig. (1) for different Λ^* at volume-fraction $\eta = 0.445$. Note that for the classical HS system ($\Lambda^* = 0$) the transition point, $\eta_c = 0.509$. As Λ^* increases the η_c decreases [33] as for $\Lambda^* = 0.1016$, $\eta_c = 0.445$ [23]. In the inset we show $S(q)$ for the same Λ^* values for comparison with $\tilde{S}(q)$. Compared to the quantum structure

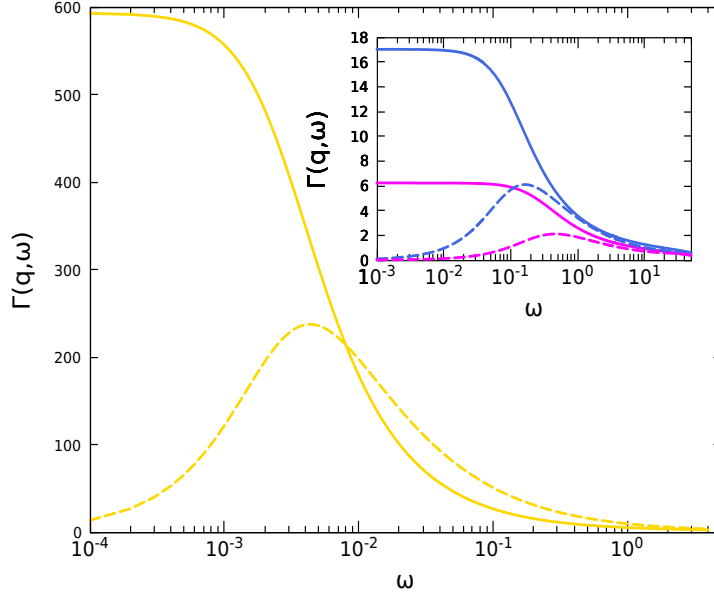


Figure 2: Real (solid curve) and imaginary (dashed curve) parts of $\Gamma(q, \omega)$ are shown for $\Lambda^* = 0.095$ (yellow) at $q = 7.11$ with frequency (in units of $1/\tau$). Inset shows the real and imaginary part of $\Gamma(q, \omega)$ for $\Lambda^* = 0.0587$ (blue) and $\Lambda^* = 0.0065$ (pink) at $q = 7.11$.

factor, $\tilde{S}(q)$ varies significantly with Λ^* ; $\tilde{S}(q)$ decreases at larger q -values due to increasing quantum uncertainty in the particle position as Λ^* is increased, while $S(q)$ approaches to 1.

$S(q)$ and $\tilde{S}(q)$ are used as inputs to solve the dynamic Eq. (6) to compute the normalized longitudinal viscosity, $\Gamma(q, \omega)$ defined in Eq. (3). In Fig. (2), the real (solid curve) and imaginary (dashed curve) parts of $\Gamma(q, \omega)$ are plotted against frequency ω (in units of $1/\tau$, where $\tau = \sqrt{m\sigma^2\beta}$) at $q = 7.11$ (first peak in $S(q)$) for $\eta = 0.445$ and $\Lambda^* = 0.095$. For comparison, results for $\Lambda^* = 0.0587$ (blue) and $\Lambda^* = 0.0065$ (pink) are shown in the inset. An increase in Λ^* leads to increase in viscosity which results in slower relaxation of density fluctuations [23]. The peak position in $\text{Im}\Gamma(q, \omega)$ shifts to low frequency regime indicating that the system is able to sustain shear stress at low frequencies and respond in a solid-like manner. The value of $\text{Re}\Gamma(q, \omega = 0)$ rises with increasing Λ^* showing an increase in viscosity and a tendency to approach the liquid-glass transition.

We use these viscosity results to compute the specific heat using Eq. (2). To analyze the specific heat spectra, the real and the imaginary parts of the frequency-dependent specific heat are plotted in Fig. (3) for different degrees of quantumness. The real and the imaginary parts of specific heat, respectively, give information on how an energy fluctuation propagates

and relaxes (dissipates) in the liquid. A peak in the imaginary part at a certain frequency denotes time-scale of the modes contributing most to the energy dissipation. These are the modes responsible for a non-zero specific heat of the supercooled liquid as most of the heat is used in the excitation of those modes. The frequency dependence of specific heat corresponding to $\Lambda^* = 0.0065$ is similar to that of the classical one (shown with black dots) and represents the classical limit of quantum specific heat. The peak position in the imaginary part of the specific heat, which corresponds to the relaxation process, shifts to the lower frequency values with increasing degree of quantum fluctuation, indicating an increasing contribution coming from the slower modes. Thus similar to the classical case when the density is increased, in quantum case too, the higher frequency modes tend to freeze first as the quantumness is increased in the supercooled regime. Inset in the lower panel shows appearance of secondary peak at high frequency regime $150 \leq \omega \leq 300$. The

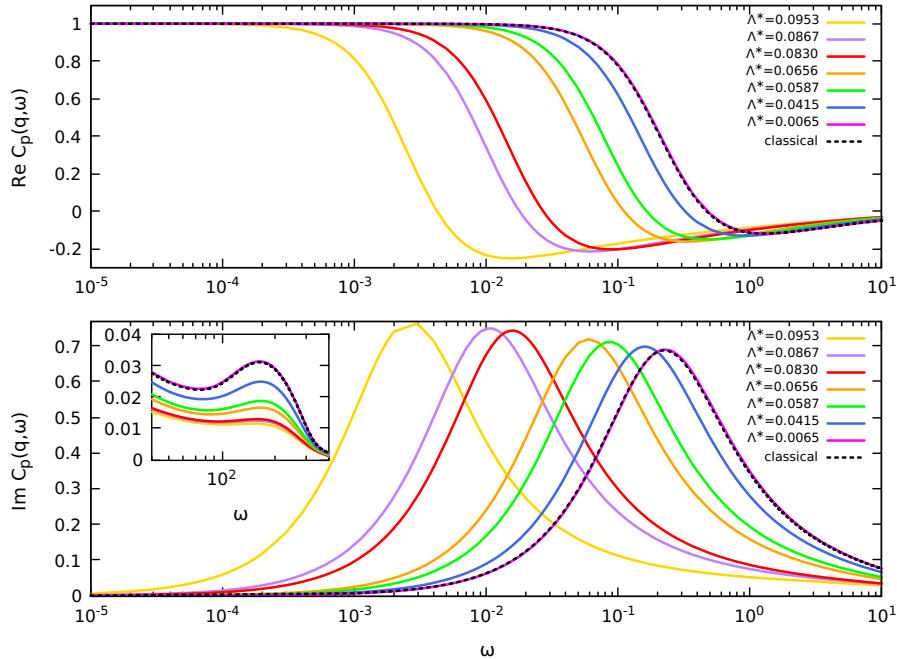


Figure 3: Real (upper panel) and imaginary parts (lower panel) of frequency-dependent specific heat of quantum HS supercooled liquid at volume-fraction $\eta = 0.445$ and $q = 7.11$ is plotted with frequency (in units of $1/\tau$) for $\Lambda^* = 0.0953$ to $\Lambda^* = 0.0065$ (from left to right). The dotted curve represents specific heat of the classical ($\Lambda^* = 0.0$) HS supercooled liquid which overlaps with the quantum result for $\Lambda^* = 0.0065$ (pink). With increasing Λ^* the peak of the imaginary part in specific heat shifts towards the lower-frequency regime. Inset in the lower panel shows a secondary peak in $\text{Im}C_p(q, \omega)$ around high frequency window ($150 - 300$).

high frequency secondary peak in the specific heat results from the short time dynamics dominated by the characteristic sound mode of frequency Ω_q [12]. As the characteristic frequency Ω_q at $q = 7.11$ does not vary with the quantumness of the system, the secondary peak position remains invariant with changing Λ^* .

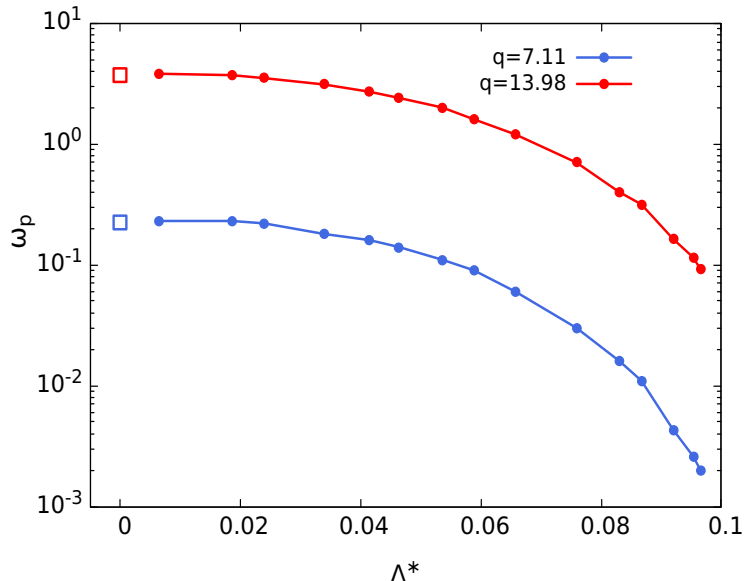


Figure 4: Peak position (ω_p) in the imaginary part of the frequency-dependent specific heat for supercooled liquid at $\eta = 0.445$ for varying degree of quantumness (Λ^*). The red and the blue curves represent shifts in the peak position for $q = 7.11$ and $q = 13.98$, respectively. Red and blue void-squares at $\Lambda^* = 0$ denote results for the classical liquid.

In Fig. (4) the peak position (ω_p) of specific heat is plotted with increasing degree of quantumness for two different q -values. For both q -values, ω_p shifts towards lower frequency regime as Λ^* increases. Different frequency modes contribute to the specific heat at different length scales. The modes contributing at $q = 7.11$ have frequency approximately an order of magnitude lower than modes contributing at $q = 13.98$ (second peak in $S(q)$). Similar to the classical case [16], in the quantum case also there is shift in the peak position of the specific heat towards the lower frequencies as the transition point is approached. It is important to compare the nature of this ω_p shift in quantum and classical supercooled liquids. We compute the shift in ω_p in both classical and quantum liquids by varying the density.

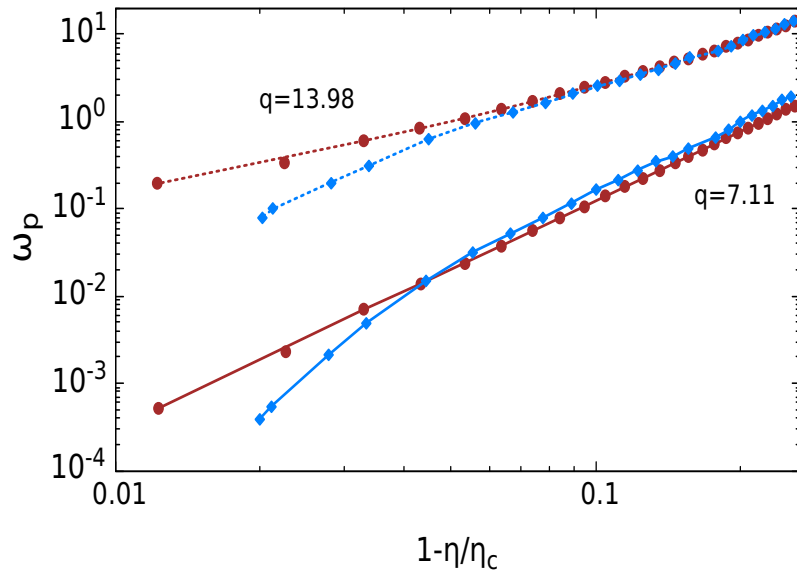


Figure 5: The peak position (ω_p) in the imaginary part of the specific heat for supercooled liquid as function of $1 - \frac{\eta}{\eta_c}$. Brown and blue curves represent results for the classical and the quantum liquids ($\Lambda^* = 0.083$), respectively, at $q = 7.11$ (bold curve) and at $q = 13.98$ (dashed curve).

In Fig. (5), we compare results for the classical (brown) and quantum (blue) liquids for wave-vectors $q = 7.11$ (bold curve) and $q = 13.98$ (dashed curve). At lower densities (far from the transition point), ω_p for both the classical and quantum liquids has similar values and shows similar decreasing trend as the density is increased. However, close to the transition point the decreasing trend in ω_p for the quantum liquid is qualitatively different from the classical case and shows much faster decay as the density is increased, indicating dominant dynamical quantum effects at higher densities.

IV. CONCLUSION

Quantum mode-coupling theory is used to study the behavior of frequency-dependent specific heat in supercooled HS quantum liquids. The quantumness of the system strongly influences dynamical relaxation in supercooled liquids. The frequency dependence of the

specific heat is found to show significant quantum effects. The slower modes contribute more to the frequency dependence as quantumness is increased. This is the trend seen in the moderate quantum liquid and is consistent with the dynamics observed for density fluctuations. At low densities, similar frequency modes contribute to the specific heat in both the classical and the quantum supercooled liquids. Quantum signatures become more pronounced as the density is increased. Near the transition point, different frequency modes contribute to the specific heat in the two cases, modes contributing to the specific heat in quantum liquids are much slower compared to those contributing in case of classical liquid. The detailed study on the quantum effects for simple HS model system presented in this work can serve as a good guide for studying the frequency dependence of specific-heat in real systems, for example, low mass colloidal systems (which show hard-sphere like behavior), where quantum effects play important role at low temperatures.

In the present calculation, the quantum effects are included using perturbative method valid in the moderate quantum regime. It will be interesting to explore the dynamical effects also in the strong quantum regime using non-perturbative approach. We plan to study this in the future.

Acknowledgments

AD acknowledges support from University Grants Commission (UGC), India. UH acknowledges Science and Engineering Research Board, India for support under the Grant No. CRG/2020/001110, and TATA Trust Travel Fund from IISc. KM acknowledges support by Japan Society for the Promotion of Science (JSPS) KAKENHI (No. 16H04034 and 20H00128).

Data Availability

The data that support the findings of this study are available from the corresponding author upon reasonable request.

[1] R. J. Speedy, *J. Phys. Chem. B* **103**, 8128 (1999).

- [2] P. G. Debenedetti, *Metastable Liquids: Concepts and Principles* (Princeton University Press, 1996).
- [3] C. A. Angell and W. Sichina, *Annals of the New York Academy of Sciences* **279**, 53 (1976).
- [4] N. O. Birge, *Phys. Rev. B* **34**, 1631 (1986).
- [5] Y. Chua, G. Schulz, E. Shoifet, H. Huth, R. Zorn, J. Smelzer, and C. Schick, *Colloid Polym Sci* **292**, 1 (2014).
- [6] E. Tombari, C. Ferrari, G. Salvetti, and G. P. Johari, *Phys. Rev. B* **78**, 144203 (2008).
- [7] W. Kauzmann, *Chemical Reviews* **43**, 219 (1948).
- [8] L. Berthier, P. Charbonneau, D. Coslovich, A. Ninarello, M. Ozawa, and s. Yaida, *Proc. Natl. Acad. Sci. U.S.A.* **114**, 11356 (2017).
- [9] N. O. Birge and S. R. Nagel, *Phys. Rev. Lett.* **54**, 2674 (1985).
- [10] D. W. Oxtoby, *J. Chem. Phys* **85**, 1549 (1986).
- [11] R. Zwanzig, *J. Chem. Phys* **88**, 5831 (1988).
- [12] S. P. Das, *Statistical Physics of Liquids at Freezing and Beyond* (Cambridge University Press, 2011).
- [13] B. Kim and G. Mazenko, *Adv. Chem. Phys.* **78**, 129 (1990).
- [14] D. R. Reichman and P. Charbonneau, *J. Stat. Mech.* **2005**, P05013 (2005).
- [15] W. Gotze and L. Sjogren, *Rep. Prog. Phys.* **55**, 241 (1992).
- [16] U. Harbola and S. P. Das, *Phys. Rev. E* **64**, 046122 (2001).
- [17] R. C. Zeller and R. O. Pohl, *Phys. Rev. B* **4**, 2029 (1971).
- [18] M. M. . B. M. Jean-François Berret, *Z. Phys. B - Condensed Matter* **87**, 213 (1992).
- [19] G. P. Silvio Franz, Thibaud Maimbourg and A. Scardicchio, *Proc. Natl. Acad. Sci. U.S.A.* **116**, 13768 (2019).
- [20] W. Götze and M. Lücke, *Phys. Rev. B* **13**, 3825 (1976).
- [21] E. Rabani and D. R. Reichman, *J. Chem. Phys* **116**, 6271 (2002).
- [22] S. Saito and B. Bagchi, *J. Chem. Phys.* **150**, 054502 (2019).
- [23] A. Das, E. Rabani, K. Miyazaki, and U. Harbola, *J. Chem. Phys.* **154**, 014502 (2021).
- [24] J.-P. Hansen and I. R. McDonald, *Theory of Simple Liquids* (Academic Press, Oxford, 2013), fourth edition ed., ISBN 978-0-12-387032-2.
- [25] K. Renziehausen and I. Barth, *Prog. Theor. Exp. Phys.* **2018** (2018), 013A05.
- [26] I. Yokoyama and Y. Waseda, *High Temp. Mater. Processes (London)* **21**, 321 (2002).

- [27] T. Itami and M. Shimoji, *J. Phys. F: Met. Phys.* **14**, L15 (1984).
- [28] T. E. Markland, J. A. Morrone, K. Miyazaki, B. J. Berne, D. R. Reichman, and E. Rabani, *J. Chem. Phys* **136**, 074511 (2012).
- [29] D. Chandler and P. G. Wolynes, *J. Chem. Phys* **74**, 4078 (1981).
- [30] F. Barocchi and U. Bafle, *Phys. Rev. E* **87**, 062133 (2013).
- [31] W. G. U Bengtzelius and A. Sjolander, *J. Phys. C: Solid State Phys.* **17**, 5915 (1984).
- [32] J. K. Percus and G. J. Yevick, *Phys. Rev.* **110**, 1 (1958).
- [33] T. E. Markland, J. A. Morrone, B. J. Berne, K. Miyazaki, E. Rabani, and D. R. Reichman, *Nature Physics* **7**, 134 (2011).